Dynamic Properties of the Intestinal Ecosystem Call for Combination Therapies, Targeting Inflammation and Microbiota, in Ulcerative Colitis

Maarten van de Guchte, Stanislas Mondot, Joël Doré

Gastroenterology 2021;161:1969–1981

Dynamic Properties of the Intestinal Ecosystem Call for Combination Therapies, Targeting Inflammation and Microbiota, in Ulcerative Colitis

Maarten van de Guchte,[1] Stanislas Mondot,[1] and Joël Doré[1,2]

[1]University Paris-Saclay, INRAE, AgroParisTech, Micalis Institute, Jouy-en-Josas, France; and [2]University Paris-Saclay, INRAE, Metagenopolis, Jouy-en-Josas, France

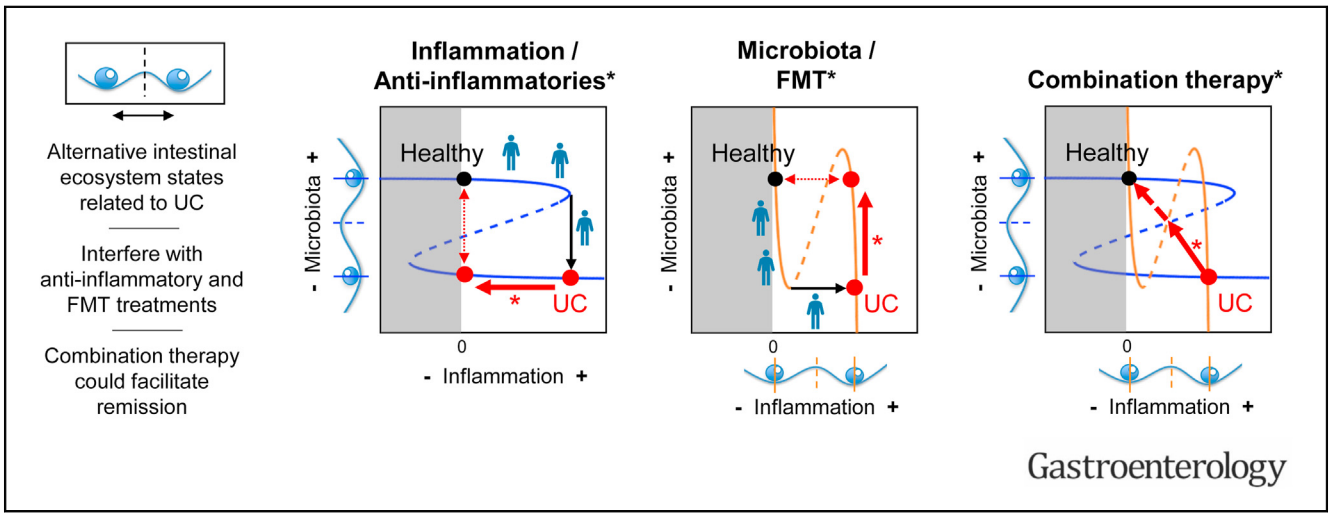

BACKGROUND & AIMS: Intestinal microbiota-host interactions play a major role in health and disease. This has been documented at the microbiota level ("dysbiosis" in chronic immune-mediated diseases) and through the study of specific bacteria-host interactions but rarely at the level of intestinal ecosystem dynamics. However, understanding the behavior of this ecosystem may be key to the successful treatment of disease. We recently postulated that health and disease represent alternative stable states of the intestinal ecosystem (different configurations that can exist under identical external conditions), which would require adapted strategies in disease treatment. Here, we examine if alternative stable states indeed exist in this ecosystem and if they could affect remission from ulcerative colitis (UC). **METHODS:** We analyzed data from a study on pediatric UC. The data reflect current treatment practice following the recruitment of treatment-naive patients with new-onset disease. Patients received personalized anti-inflammatory treatments over a period of 1 year. Stool samples at 0, 4, 12, and 52 weeks allowed an estimation of microbiota status (through 16S ribosomal RNA gene sequencing) and host inflammatory status (through the measurement of fecal calprotectin levels). **RESULTS:** We identify 4 microbiota states and 4 host states. Longitudinal data show that the improvement of inflammatory status is accompanied by an improvement of microbiota status. However, they also provide strong indications that both improvements are retarded or blocked by alternative states barriers. **CONCLUSIONS:** Our observations strongly suggest that inflammation suppression should be combined with microbiota management where possible to improve the efficacy of UC treatment.

Keywords: Alternative Stable States; GI Tract; Microbiota; Host; Symbiosis.

The intestinal microbiota plays a role of increasingly recognized importance in human health through its impact on fundamental host processes, notably including the modulation of the innate immune system. The host, in turn, controls the microbiota, and reciprocal microbiota-host influences constitute the basis for the establishment of a relatively stable state of equilibrium in the intestinal ecosystem.[1]

There is reason to believe that this equilibrium can take different forms representing so-called alternative

Abbreviations used in this paper: **FMT, fecal microbiota transplantation; OTU, operational taxonomic unit; PCoA, principal coordinates analysis; rRNA, ribosomal RNA; T0, week 0; T4, week 4; T12, week 12; T52, week 52; UC, ulcerative colitis.**

Most current article

0016-5085
https://doi.org/10.1053/j.gastro.2021.08.057

WHAT YOU NEED TO KNOW

BACKGROUND AND CONTEXT

Ulcerative colitis (UC) is characterized by a deregulated innate immune system and a modified intestinal microbiota; it is notoriously difficult to cure. These characteristics are reminiscent of the altered function and restricted dynamics properties of alternative stable (eco)system states.

NEW FINDINGS

We provide, to our knowledge, the first formal proof for the existence of alternative stable states of the human intestinal ecosystem. Our analyses strongly suggest that the stability of these states interferes with remission from UC under the standard of care. They may also explain the variable success of fecal microbiota transplantation in the treatment of UC.

LIMITATIONS

This study considers intrinsic properties of the intestinal ecosystem: microbiota and host inflammatory status. For disease remediation, external factors (eg, diet) need to support a healthy ecosystem state.

IMPACT

New insights from this study provide a strong rationale for the application of combinatorial therapeutic strategies, combining anti-inflammatory treatments and microbiota management, in UC.

stable states (Figure 1*A*)[2] that can exist under identical conditions (Figure 1*B*) (as opposed to condition-dependent states [Figure 1*C*]). Alternative stable state dynamics have been described for several complex (eco-)systems, ranging from lakes and oceans to tropical forests: although a rapid catastrophic[3] transition to an alternative state may be provoked when conditions change beyond the limit of robustness of the current state (a tipping point), simply setting the conditions back to what they were would not revert the system state to its initial configuration (if the initial conditions are within the bistable range [Figure 1*B*]).[3] This becomes important when alternative intestinal ecosystem states condition health or chronic disease, as we postulate that they do.[1] Alternative states associated with inflammatory bowel diseases could (partly) explain the notorious difficulty in curing these diseases, where drug efficacy has reached a plateau.[4] If these hypotheses prove true, they will profoundly affect disease management while, at the same time, opening conceptually new avenues for prevention and therapy.[2]

We recently provided a proof of concept for the existence of alternative stable states of the intestinal ecosystem in a rat model of dextran sodium sulfate–induced colitis (a model for ulcerative colitis [UC][5]).[2] In this study, we address the question of whether alternative stable states can be detected in the human intestinal ecosystem in a context of pediatric UC. We show that alternative intestinal ecosystem states indeed exist and, because of their stability, likely delay or prevent remission from UC.

Methods

The experimental setup, data collection, and initial treatment of 16S ribosomal RNA (rRNA) gene sequence data are described in the original publication by Schirmer et al.[6] Briefly, 428 treatment-naive pediatric patients with new-onset UC were recruited from 29 centers in the United States and Canada. They were assigned to receive 1 of 2 conventional treatment strategies: (1) 5-aminosalicylic acid (mesalamine) or (2) oral/intravenous corticosteroids followed by mesalamine; they were monitored over the course of 1 year. Treatment strategies were based on disease severity and progression. As part of this study, stool samples were collected at baseline (week 0 [T0]) and 1 or more follow-up timepoints (approximately 4 [T4], 12 [T12], and 52 [T52] weeks after initial treatment initiation) and were used for microbiome profiling (16S rRNA gene sequencing) and fecal calprotectin measurement. Metadata included antibiotics use, disease severity category, and remission status. Participants were between 4 and 17 years of age (mean age, 12.8 ± 3.3 years), and 48% were female. Eligibility criteria for patients were disease extent beyond the rectum (ie, proctitis excluded), a baseline Pediatric UC Activity Index[7] score of at least 10, no previous therapy for colitis, and negative stool culture results for enteric bacterial pathogens (*Salmonella*, *Shigella*, *Campylobacter*, and *Escherichia coli* 0157:H7) and *Clostridium difficile* toxin.

The data used in this study were retrieved in the form of an OTU table for fecal microbiota samples, fecal calprotectin levels, and relevant metadata. Combined microbiota-calprotectin information was available for 881 stool samples from 367 patients. For longitudinal analyses, samples from patients who had used antibiotics within a period of 27 days before stool sample collection were excluded (leaving 805 samples from 353 patients). Data analysis methods used are specified in the main text and figure legends.

Data Availability

The data used in this study are available as supplementary information accompanying the original publication by Schirmer et al.[6]

Ethics Approval

The clinical data used in this study (fecal microbiome and calprotectin data as well as metadata) were collected and published with an ethics statement by Schirmer et al.[6]

Results

Intestinal Microbiota and Host Inflammatory Status in Ulcerative Colitis

To investigate if alternative stable states can be distinguished in the human intestinal ecosystem, we analyzed existing data from a study on pediatric patients with UC.[6] This data set presents a number of features that are of particular interest for our study: (1) The study recruited treatment-naive patients with UC, and the first set of data was collected before any medical treatment; (2) The data provide simultaneous estimations of intestinal microbiota status, through 16S rRNA gene sequencing of stool samples, and host status, through the measurement

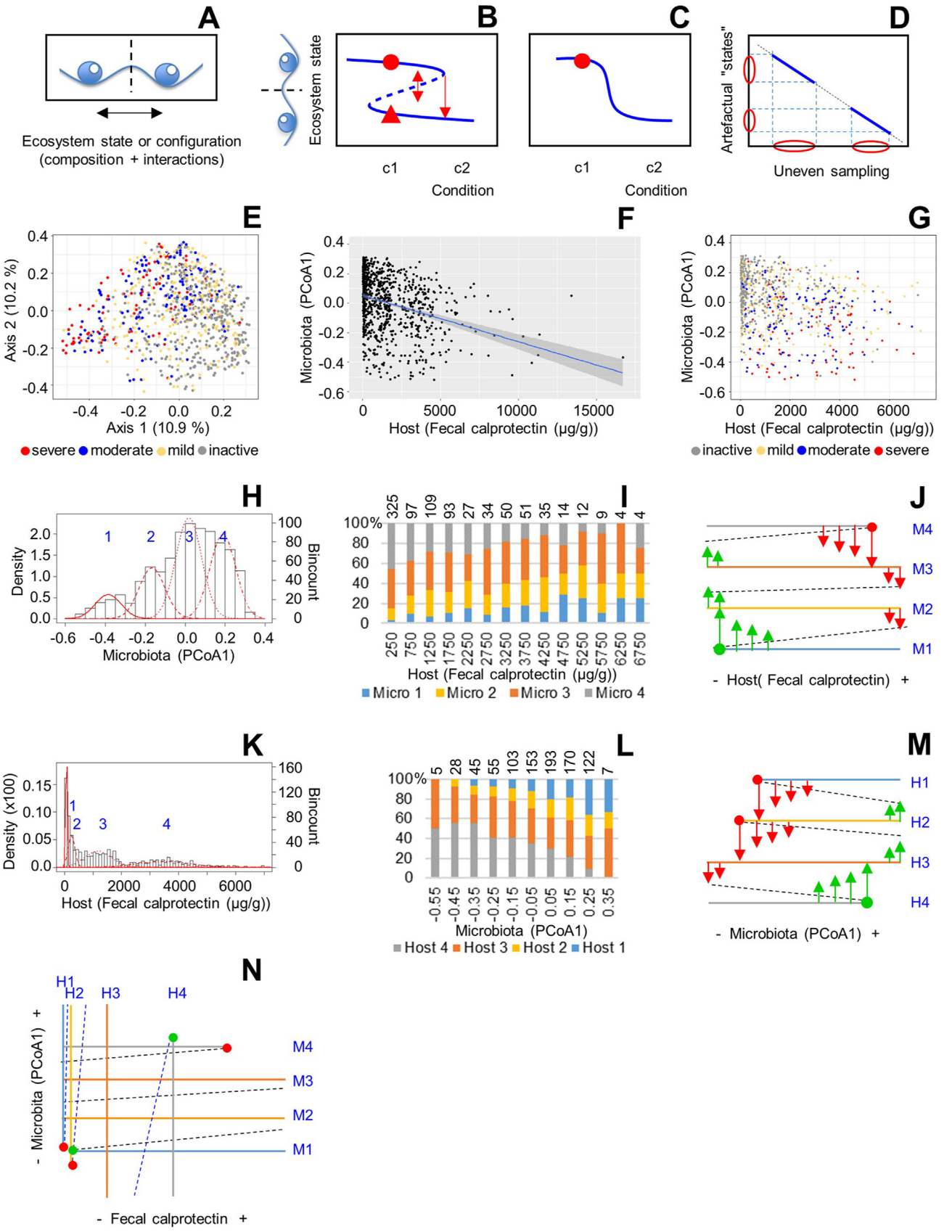
A
Ecosystem state or configuration
(composition + interactions)
B
Ecosystem state
c1
c2
Condition
C
c1
c2
Condition
D
Artefactual "states"
Uneven sampling
E
Axis 2 (10.2 %)
Axis 1 (10.9 %)
severe moderate mild inactive
F
Microbiota (PCoA1)
Host (Fecal calprotectin (µg/g))
G
Microbiota (PCoA1)
Host (Fecal calprotectin (µg/g))
inactive mild moderate severe
H
Density
Biocount
Microbiota (PCoA1)
I
Host (Fecal calprotectin (µg/g))
Micro 1 Micro 2 Micro 3 Micro 4
J
M4
M3
M2
M1
- Host(Fecal calprotectin) +
K
Density (x100)
Biocount
Host (Fecal calprotectin (µg/g))
L
Microbiota (PCoA1)
Host 4 Host 3 Host 2 Host 1
M
H1
H2
H3
H4
- Microbiota (PCoA1) +
N
H1
H2
H3
H4
M4
M3
M2
M1
- Microbita (PCoA1) +
- Fecal calprotectin +

of fecal calprotectin levels (a human inflammation marker shown to correlate with endoscopic disease activity scores like the Ulcerative Colitis Endoscopic Index of Severity[8] or Mayo Endoscopic Score[9] and histologic remission vs activity[10]); (3) The study cohort includes patients with varying degrees of disease severity, ensuring the variation in microbiota status and host status needed for our analyses; and (4) The patients were followed up over a period of 1 year, with additional sampling at 4, 12, and 52 weeks after the initiation of anti-inflammatory medication.

Moreover, the cohort reflects the current standard of care, where anti-inflammatory medication depends on the initial diagnosis and is subsequently adapted to the evolution of the patient's clinical picture.

Regarding microbiota, a principal coordinates analysis (PCoA) of 16S rRNA gene profiles shows a gradient of partially overlapping disease severity classes[6,7] on the first axis (Figure 1*E* and Supplementary Figure 1, axis 1 [PCoA1]). will therefore use the position on PCoA1 as the univariate measure of microbiota status needed in subsequent analyses. (A detailed taxonomic analysis of microbiota composition as a function of disease severity can be found in the original publication.[6]) When microbiota status is plotted against host inflammatory status (fecal calprotectin level), thus positioning participants according to intestinal ecosystem status, a correlation between the 2 is observed (Figure 1*F* and *G*), coherent with the overwhelming evidence of reciprocal impact reported in the literature.

Four Alternative Microbiota States

Microbiota status (PCoA1 value) shows a nonnormal distribution (Figure 1*H* and Supplementary Figure 2*A*–*C*). Finite Gaussian mixture modeling strongly suggests a mixture of 4 normal distributions, implicating 4 microbiota states (M1–M4). To discriminate among the possibilities that these states represent alternative stable states

Figure 1. Alternative microbiota and host states. (*A*) Alternative stable states of an ecosystem as beads in a stability landscape. The dashed line represents the frontier between 2 basins of attraction (transition fold). (*B*) Alternative states (solid lines) can both exist under a range of identical conditions (bistable range). Dashed line, see *A*. The width and shape of the basins of attraction—and thereby the stability of the alternative states and likelihood of transitions across the transition fold (due to stochastic movements, *red bidirectional arrow*)—change with changing conditions, as illustrated by the changing distances between the solid lines and dashed line.[3] When changing conditions push the ecosystem beyond a tipping point (*sharp bend in the Z-shape curve*) where the basin of attraction of its present state disappears, it rapidly transits to an alternative state (*red arrow*). (*C*) Condition-dependent states. Assuming that the original ecosystem state is represented by the red dot, the models from *B* and *C* both predict a change of ecosystem state when the external conditions change from c1 to c2. When the conditions change back to c1, the model in *B* predicts that the system remains in the alternative state (*red triangle*), whereas the model in *C* predicts that the system returns to its original state. (*D*) Uneven sampling (indicated by *red ellipses*) of a system with a linear relationship between ecosystem state and condition could give a false impression of the existence of alternative ecosystem states. Alternative stable states (*B*) can be distinguished from condition-dependent states (*C*) and uneven sampling artifacts (*D*) by the distribution of the ecosystem state in subgroups with a similar condition. Mixed normal distributions are expected in several subgroups (within the bistable range) in *B*, whereas distributions close to normal are expected in each subgroup in *C* and *D*. (*E*) PCoA of ecologic distances between microbiota samples (Bray-Curtis distance OTU data as made available in Schirmer et al[6] from all stool samples for which calprotectin data are also available [n = 881 samples from 367 patients]). Colors indicate disease severity classes.[6,7] (*F*) Microbiota status (position on the PCoA1 axis from *E*) vs host inflammatory status (fecal calprotectin level). The blue line shows correlation (rho = –0.355; $P < 2.2e{-}16$ by Spearman rank correlation test; the grey area represents the standard error). (*G*) Zoomed in on the left part of *F*. Colors indicate disease severity classes. (*H*) Multimodal distribution of microbiota status. PCoA1 coordinates from the ordination plot in *E* as a measure of microbiota status are divided in categories with a range of 0.05, and the frequency of occurrence of each category is plotted (bincount). Shapiro test for normality: $P = 1.2e{-}14$ (ie, not a normal distribution). Mixed normal distribution density overlay with 4 components (*red*) according to finite Gaussian mixture modeling using mclust 5.4[18] (maximal value of the Bayesian information criterion corroborated by bootstrap sequential likelihood ratio testing; $P = .001$). (*I*) Relative frequencies of alternative microbiota states (*H*) as a function of host inflammatory status. Relative frequencies are calculated from the data in *G*. A weight between 0 and 1 is attributed to each observation using probabilities of belonging to a given microbiota state calculated by mclust (*H*). Host inflammatory status. Fecal calprotectin levels are binned in intervals of 500 μg/g; the central value of each bin is indicated. Numbers at the top of the graph indicate the number of observations in each bin. (*J*) Schematic representation of microbiota states (*solid lines*) and transition folds (*dashed lines*) as a function of host inflammatory status. Arrows indicate transitions that become more probable as inflammation increases (*red*) or decreases (*green*) and basins of attraction contract (compare with *B*). Red and green dots indicate tipping points. (*K*) Multimodal distribution of host status. Fecal calprotectin levels as a measure of host inflammatory status are divided in categories with a range of 100 μg/g, and the frequency of occurrence of each category is plotted (bincount). Shapiro test for normality: $P = 2.2e{-}16$. Mixed normal distribution density overlay with 4 components (*red*) according to finite Gaussian mixture modeling using mclust 5.4 with manual adjustment (Supplementary Figure 2*E* and *F*). (*L*) Relative frequencies of alternative host states (*K*) as a function of microbiota status. Relative frequencies are calculated from the data in *G*. A weight between 0 and 1 is attributed to each observation using probabilities of belonging to a given host state calculated by mclust (*K*). Microbiota status, PCoA1 value (*G*) binned in intervals of 0.1; the central value of each bin is indicated. Numbers at the top of the graph indicate the number of observations in each bin. (*M*) Schematic representation of host states (*solid lines*) and transition folds (*dashed lines*) as a function of microbiota status. Arrows indicate transitions that become more probable as microbiota PCoA1 value decreases (*red*) or increases (*green*) (compare with *B*). Red and green dots indicate tipping points. (*N*) The superposition of *J* and *M*. Intersections of stable microbiota states and stable host states represent stable intestinal ecosystem states.

(Figure 1*B*), condition- (inflammation)-dependent states (Figure 1*C*), or artifacts because of uneven sampling (Figure 1*D*), we analyzed their distribution in subgroups of individuals with similar inflammatory status. The results of this analysis show that all 4 microbiota states are represented in nearly every subgroup (Figure 1*I*). Multimodality of microbiota status distributions was confirmed in independent analyses (not relying on projection of the overall microbiota status distribution shown in Figure 1*H*) of subgroups of 100 samples grouped by host inflammatory status (Supplementary Table 1). Together, these observations clearly invalidate the condition-dependent states and uneven sampling artifact models.

Individual patients can move from one state to another over time (as is discussed later), indicating that the microbiota states do not represent static subpopulations. The relative contribution of microbiota state M4 diminishes with increasing host inflammatory status (increasing fecal calprotectin levels) (Figure 1*I* and Supplementary Figure 2*D*), consistent with a contracting basin of attraction and indicating the approach of a tipping point where this state disappears (approximately 5000 μg calprotectin/g) (Figure 1*I* and *J*; compare with the legend for Figure 1*B*). Microbiota state M1 shows the opposite behavior, with a predicted tipping point near the lower end of the host inflammation scale (approximately 500 μg calprotectin/g). The relative contributions of microbiota states M2 and M3 seem less or not affected by host inflammatory status (Supplementary Figure 2*D*), likely because of the fact that these states are affected by transitions (across transition folds) (Figure 1*B*) to and from 2 adjacent states, the numerical effects of which may annul each other. In 1-to-1 comparisons with adjacent states, however, the relative contributions of these states do change as a function of inflammatory status. Unlike states M1 and M4, the representation of states M2 and M3 never approached 0, indicating that the tipping points where these states would disappear are located outside of the presented calprotectin range (ie, at inaccessible negative calprotectin values for the left-hand tipping points).

Taken together, these observations show that the different microbiota states can be considered as alternative stable states. Microbiota state M1 is predicted to disappear if inflammation can be reduced to a very low level (Figure 1*J*). Microbiota states M2 and M3 are not expected to disappear even under those favorable conditions. In other words, the more favorable (see section on "Alternative Ecosystem States in Treatment-Naive Individuals") microbiota state M4 will not be automatically reached in all patients, even if inflammation is reduced to close to 0. Rather, the instauration of a new equilibrium is expected among patients in microbiota states M2, M3, and M4 (Figure 1*I*), depending on the size and shape of their respective basins of attraction and transitions across transition folds due to stochastic movements (Figure 1*B*). Microbiota state M4 is set to disappear, and is not easily restored, when inflammation levels (temporarily) become high, followed by states M3 and M2 when inflammation continues to increase.

Four Alternative Host States

Host inflammatory status, as assessed by fecal calprotectin levels, is not normally distributed either (Figure 1*K*). Finite Gaussian mixture modeling with manual adjustment (Supplementary Figure 2*E* and *F*) suggests the existence of 4 host states, H1–H4 (Figure 1*K* and Supplementary Figure 2*G–I*). The 4 host states can be recognized in nearly all subgroups of individuals with similar microbiota status (PCoA1) except those at the extremities of the PCoA1 scale, be it in analyses using projections of the overall distribution of host status (Figure 1*L*) or in independent analyses of subgroups of 100 samples grouped by microbiota status (Supplementary Table 2).

The relative contribution of host state H4 (high inflammation levels) diminishes with increasing microbiota PCoA1 value before disappearing (Figure 1*L* and Supplementary Figure 2*J*), indicating that a tipping point is reached (near PCoA 0.3) (Figure 1*L* and *M*). Host states H1 and H2 show the opposite behavior, with predicted tipping points at the lower end of the microbiota PCoA1 scale (near PCoA −0.4 and −0.5, respectively). Intermediate host state H3 represents a nearly constant fraction of observations in each subgroup of participants, but in 1-to-1 comparisons with adjacent states, the relative contribution of this state also changes as a function of microbiota status. Tipping points for this state and the right-hand tipping point for state H2 are located outside of the presented microbiota range.

Figure 1*L* and *M* suggests that one might be able to drive the host out of its most inflammatory state H4, and only out of this state, if one could successfully restore the essential components of a healthy microbiota (ie, when acting only on the microbiota parameter of the ecosystem to increase PCoA1). If applied to a large number of patients, the proportions of patients in the other host states (H1 [no inflammation] to H3) are expected to change (Figure 1*L*, *right*), which in practice would translate to variable success of microbiota engineering. Alternative states could thus explain the variable success of an extreme form of microbiota engineering: fecal microbiota transplantation (FMT) from a healthy donor.[11,12] Inversely, deterioration of the microbiota is expected to lead to a deterioration of intestinal health (inflammation) that will be difficult to reverse, owing in part to mutually sustaining mechanisms.

Alternative Ecosystem States in Treatment-Naive Individuals

From the existence of alternative stable host and microbiota states with their respective basins of attraction (Figure 1*A*), it follows that individuals are predominantly expected at the intersections of these states in the microbiota-vs-host status plot (Figure 1*N*). These intersections represent alternative stable states of the intestinal ecosystem as a whole.[2] This pattern can indeed be recognized in a density plot (Figure 2*A* and *B*). Importantly, it can also be recognized in treatment-naive patients (ie, at T0) (Figure 2*C*), although here, the host states with the lowest calprotectin levels (H1 and H2) are obviously very sparsely populated, and microbiota state M4 is nearly

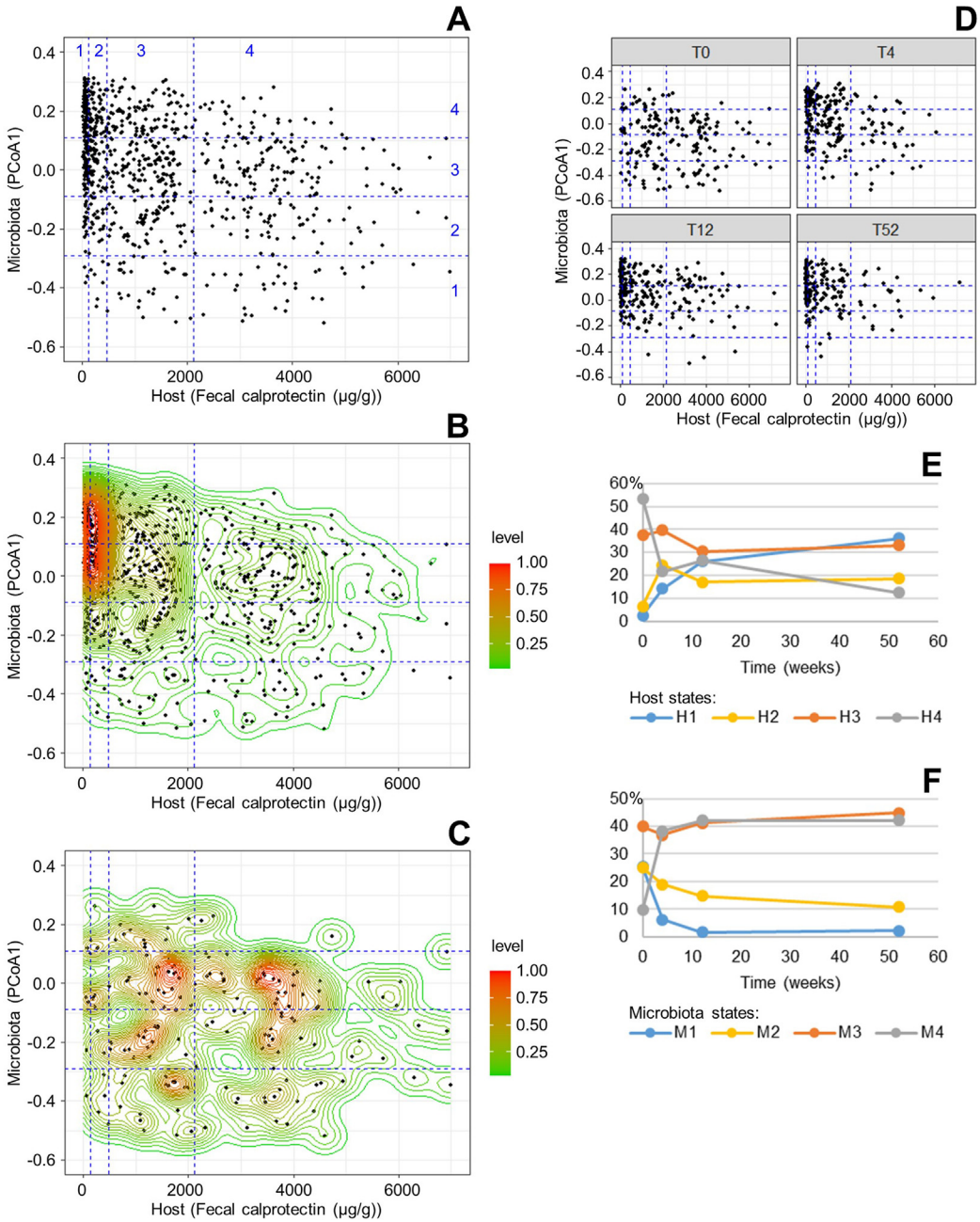

Figure 2. Alternative intestinal ecosystem states. (*A*) Microbiota status (position on the PCoA1 axis from Figure 1*E*) plotted against host inflammatory status (fecal calprotectin level). Numbers 1–4 indicate alternative microbiota states (Figure 1*H*) and alternative host states (Figure 1*K*). Positions of the dashed state separation lines correspond to positions where the density curves in Figure 1*H* or *K* intersect, that is, where the probability of belonging to either of 2 adjacent states is the same. (*B*) As in *A*, including relative density level contours estimated using ggplot2::stat_density2d. (*C*) As *B*, using only data from treatment-naive patients (T0; n = 185). (*D*) As in *A*, with separate plots for different sampling timepoints (0, 4, 12, and 52 weeks). Not all patients are represented at all timepoints; see Schirmer et al[6] for details. (*E*) Relative abundance of different host states as a function of time since treatment initiation; data from *D*. (*F*) Relative abundance of different microbiota states as a function of time since treatment initiation; data from *D*. See Supplementary Figure 7*A* for more details. Panels *C*–*F* exclude patients who had used antibiotics within a period of 27 days before stool sample collection (leaving n = 805 samples from 353 patients; n = 185 for T0).

absent. In the absence of a healthy control group among the recruited participants, we postulate that microbiota state M4 represents the healthiest microbiota state because (1) this state becomes populated after anti-inflammatory treatments (see section on "Evolution of the Microbiota Under Anti-inflammatory Pressure"), (2) a significantly higher percentage (56%) of the participants in this state at T52 are in remission than in microbiota state M3 (38%) (Supplementary Figure 3), and (3) an analysis of the taxonomic composition of the different microbiota states

Table 1. Microbiota States and Relative Genus Abundances

Phylum	Genus	M1 Mean	SD	M2 Mean	SD	M3 Mean	SD	M4 Mean	SD	Q	M1/M4	M2/M4	M3/M4	M4/M4
A	*Adlercreutzia*	2.30e–06	1.30e–05	8.70e–05	4.60e–04	2.30e–04	6.40e–04	1.20e–03	1.90e–03	2.10e–20	0.00	0.07	0.19	1.00
A	*Collinsella*	3.40e–04	1.20e–03	3.70e–03	1.40e–02	1.80e–02	4.50e–02	5.10e–02	5.70e–02	1.10e–25	0.01	0.07	0.35	1.00
F	*Anaerostipes*	3.00e–05	1.50e–04	2.80e–04	1.20e–03	1.30e–03	3.00e–03	2.00e–03	3.50e–03	8.60e–24	0.02	0.14	0.65	1.00
F	*Blautia*	2.00e–03	7.40e–03	2.50e–02	5.90e–02	5.40e–02	6.60e–02	1.00e–01	6.00e–02	5.00e–50	0.02	0.25	0.54	1.00
A	*Bifidobacterium*	5.30e–03	9.00e–03	4.30e–02	6.90e–02	7.80e–02	1.10e–01	1.60e–01	1.00e–01	8.50e–39	0.03	0.27	0.49	1.00
A	*Eggerthella*	1.40e–04	5.60e–04	2.50e–03	4.00e–03	3.10e–03	7.30e–03	3.60e–03	4.30e–03	8.30e–22	0.04	0.69	0.86	1.00
F	*Roseburia*	5.10e–05	1.80e–04	3.00e–03	1.30e–02	1.70e–03	5.00e–03	1.30e–03	3.20e–03	9.90e–16	0.04	2.31	1.31	1.00
F	*Coprococcus*	2.00e–04	5.40e–04	6.90e–04	1.20e–03	2.20e–03	5.70e–03	3.60e–03	4.70e–03	1.80e–27	0.06	0.19	0.61	1.00
F	*Dorea*	1.30e–03	4.10e–03	6.60e–03	1.50e–02	9.80e–03	1.40e–02	1.40e–02	9.70e–03	6.20e–30	0.09	0.47	0.70	1.00
F	*Faecalibacterium*	1.60e–02	4.20e–02	6.30e–02	7.10e–02	1.60e–01	1.30e–01	1.60e–01	9.70e–02	1.40e–29	0.10	0.39	1.00	1.00
P	*Eikenella*	1.40e–03	3.10e–03	7.00e–04	2.40e–03	3.50e–05	1.40e–04	6.40e–05	6.40e–04	4.20e–15	21.88	10.94	0.55	1.00
P	*Haemophilus*	1.10e–01	1.40e–01	3.00e–02	5.40e–02	2.00e–02	5.00e–02	2.00e–03	8.20e–03	1.40e–25	55.00	15.00	10.00	1.00
Fu	*Fusobacterium*	2.00e–02	3.50e–02	1.00e–02	3.50e–02	1.70e–03	1.40e–02	1.20e–04	4.70e–04	1.90e–21	166.67	83.33	14.17	1.00
F	*Veillonella*	9.60e–02	1.10e–01	2.70e–02	4.70e–02	5.70e–03	1.10e–02	4.80e–04	1.30e–03	9.30e–31	200.00	56.25	11.88	1.00
P	*Aggregatibacter*	5.30e–03	1.40e–02	1.50e–03	7.00e–03	8.70e–04	4.20e–03	2.40e–05	1.60e–04	5.90e–11	220.83	62.50	36.25	1.00
P	*Erwinia*	8.80e–02	1.80e–01	1.00e–02	3.00e–02	3.70e–03	1.90e–02	3.70e–04	1.80e–03	2.40e–17	237.84	27.03	10.00	1.00
F	*Enterococcus*	1.10e–02	4.70e–02	1.80e–03	8.70e–03	1.30e–03	1.20e–02	3.10e–05	1.20e–04	1.10e–04	354.84	58.06	41.94	1.00

NOTE. Genera for which significant relative abundance differences between microbiota states M1–M4 were observed ($Q < .01$; Kruskal-Wallis test with Benjamini-Hochberg false discovery rate correction) and for which M1/M4 was $\leq$0.1 or $\geq$10. M*n*/M4 values indicate ratios of means. Genera for which the mean relative abundance was <0.1% in all 4 microbiota states were ignored. Only microbiota samples that could be attributed to 1 of the 4 microbiota states with a probability of >95% (mclust) were taken into consideration (M1, n = 58; M2, n = 78; M3, n = 107; M4, n = 159). Green: M4-associated genera are all members of the core microbiota of healthy individuals[19] and exclusively belong to the phyla Actinobacteria and Firmicutes, reminiscent of the Firmicutes-dominated enterotype.[20,21] The observed M1/M4 ratios are consistent with the rather well-documented loss of Firmicutes in inflammatory bowel diseases[22] and a loss of the anti-inflammatory properties associated with butyrate production by dominant core Firmicutes such as *Faecalibacterium* or *Blautia* in M1 (together 26% of the relative genus abundance on average in M4 vs 1.8% in M1). Red: non–M4-associated genera are not members of the core microbiota of healthy individuals and mainly belong to the phylum Proteobacteria. They will express proinflammatory signals and are potentially associated with severe pathologies such as endocarditis or cancer.
A, Actinobacteria; F, Firmicutes; Fu, Fusobacteria; P, Proteobacteria; SD, standard deviation.

Table 2. Alternative Microbiota States and OTU Numbers

Characteristics	Microbiota states			
	M1	M2	M3	M4
Number of samples[a]	58	78	107	159
Mean number of OTUs/sample	104	156	205	208
SD	36	58	62	55
Median number of OTUs/sample	103	157	194	206

[a]Samples that are attributed to a given microbiota state with a probability of >95% (mclust).

supports this hypothesis (Table 1). This hypothesis is corroborated by the analysis of the microbiota from healthy individuals: within the set of 402 microbiota samples analyzed in Table 1, the relative abundances of the indicated genera allowed a reliable classification of samples as belonging to microbiota state M1, M2, M3, or M4 (receiver operating characteristic analysis of multiclass area under the curve models with 17 or 14 differential genera) (Supplementary Figures 4–6). When the model with 14 genera was used to classify microbiota samples from 254 healthy US citizens (125 aged 4–17 years, 129 aged 18–58 years; a data set in which only 14 of the 17 differential genera were represented),[13] 252 were classified as M4, 1 as M3 (a 46-year-old woman), and 1 as M2 (a 50-year-old man with a body mass index of 38kg/m^2) (Supplementary Figure 6*C*). This result confirms our hypothesis that state M4 represents a healthy microbiota state. Although our results indicate that states M2 and M3 can also be found in healthy individuals, their prevalence and possible predictive significance as warning signs in (risk groups of) healthy individuals need further study. Microbiota richness, a parameter considered as an important indicator of health,[14] is comparable in microbiota states M3 and M4 but considerably reduced in states M2 and M1 (Table 2).

Evolution of the Microbiota Under Anti-inflammatory Pressure

Do alternative states affect treatment success? *Treatment success* can be defined as a concomitant durable suppression of inflammation and restoration of a healthy microbiota, creating conditions where the risks of relapse are minimal. Anti-inflammatory treatments rapidly improved inflammatory status within the first 4 weeks of treatment (Figure 2*D* and *E* and Supplementary Figure 7*A*). This development was accompanied by a clear shift in microbiota status toward state M4 (Figure 2*D* and *F* and Supplementary Figure 7*A*), irrespective of treatment (either mesalamine, oral steroids, or intravenous steroids) (Supplementary Figure 7*B*). However, after 52 weeks of personalized anti-inflammatory treatments, only 36% of the patients had reached host state H1, the only state with fecal calprotectin levels (<127 μg/g) that can be considered nonpathologic.[10] Although this may in part be due to the limitations of long-term anti-inflammatory treatments, a more significant observation is that only about half of these (19% of all patients at T52) (Supplementary Figure 7*A*) had reached the most favorable, least inflammation-prone microbiota state M4. Microbiota state M1 nearly completely disappeared after 12 weeks of treatment, whereas state M3 and, to a lesser extent state, M2 persisted even after 52 weeks, including among participants where the inflammation level had fallen to close to 0 (host state H1). These observations are in agreement with the aforementioned alternative state characteristics (Figure 1*J*) and strongly deviate from what could be expected in the absence of alternative state barriers.

Individual patients' trajectories from one sampling timepoint to the next corroborate this: important reductions in inflammation were often not accompanied by a change in microbiota state in spite of very low calprotectin levels being reached (Figure 3*A*). It seems very unlikely that this would be due to microbiota response time because all time intervals (from 4 to 40 weeks) are concerned. In addition, in other cases where microbiota state transitions did take place, they were often limited to a shift to the neighboring state (Figure 3*B* and Supplementary Figure 8*A*).

One could speculate that, rather than being due to alternative state barriers, the apparent stalling of microbiota restoration at an intermediate state may reflect a prevention from access to a more favorable state because of incompatible environmental factors (eg, diet or host genetics). However, when selecting individuals who show at least at 1 timepoint a state M4 microbiota (ie, state M4 is accessible for these patients) and plotting the evolution of PCoA1 from T0 to T4 (Supplementary Figure 8*B*), we observe a similar pausing at state M3. When selecting patients for whom at least state M3 is accessible, we observe pausing at state M2 (Supplementary Figure 8*C*). These results furthermore show that pausing can be observed within a single time interval and irrespective of treatment (Supplementary Figure 8*D* and *E*).

Together, these observations indicate that alternative microbiota state properties hinder the restoration of a healthy microbiota after treatments used in the standard of care for UC.

Evolution of the Microbiota Under Inflammatory Pressure

A substantial number of patients show, for one of the time intervals, a net increase of inflammation rather than a decrease (Figure 3*C* and *D*). These observations may reflect temporary treatment interruptions or be due to surges in inflammation that could not be completely mastered or compensated by the treatment in place. Remarkably, under conditions of large net inflammation increase, the general impression is predominantly one of conservation of the microbiota state (Figure 3*C* and Supplementary Figure 8*F*), including over longer time periods (8 or 40 weeks, detail not shown), in agreement with the properties of alternative stable states documented earlier.

Two groups of observations may seem to be in contradiction with this conclusion. First, a number of vectors

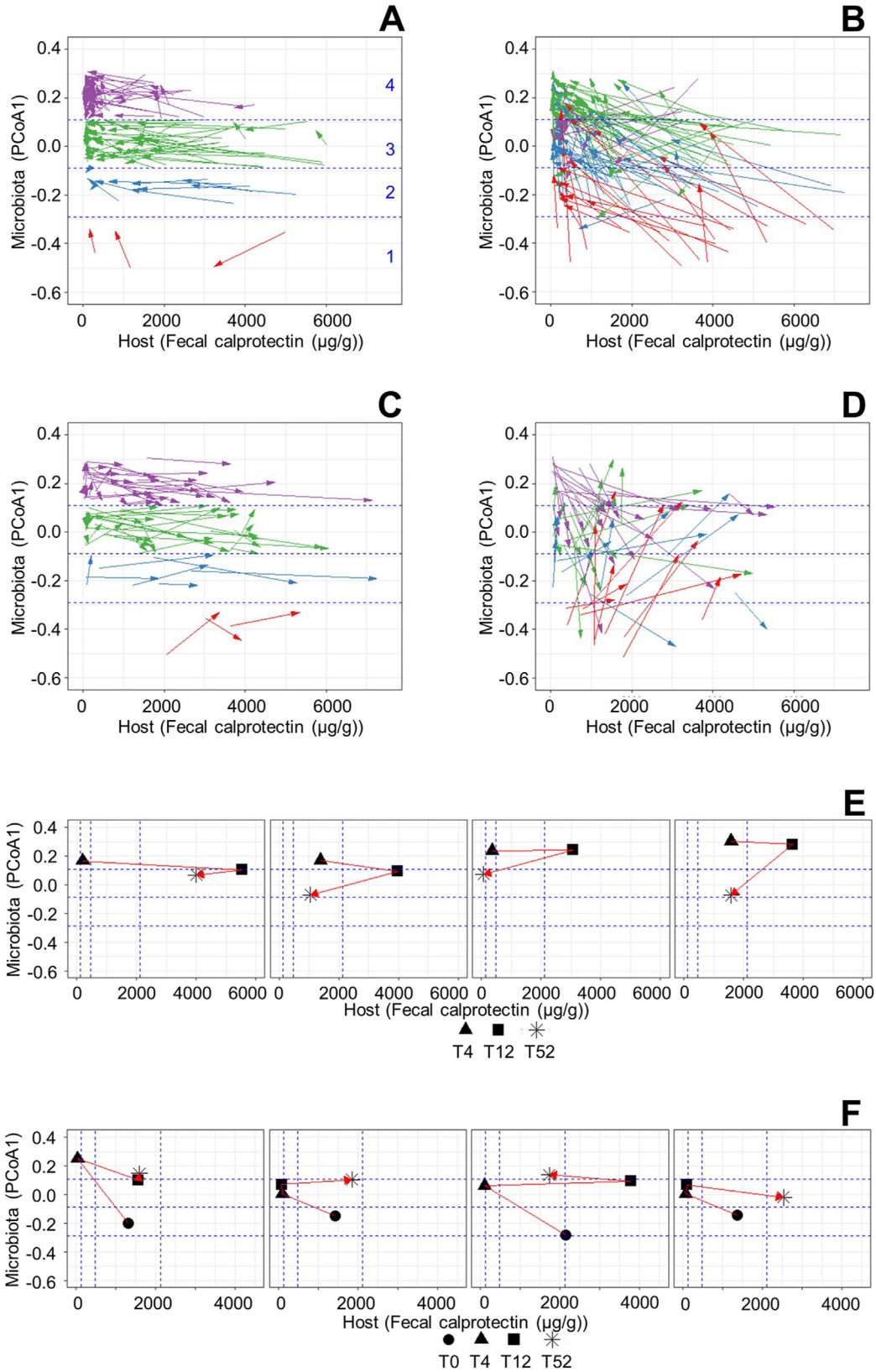

Figure 3. Evolution of individual intestinal ecosystems. Vectors indicate the evolution of the intestinal ecosystem of a given patient from one timepoint to the next (T0 to T4, T4 to T12, or T12 to T52). Alternative microbiota and host states as in Figure 2*A*. Patients who had used antibiotics within a period of 27 days before stool sample collection were excluded. (*A–D*) Colors indicate microbiota state at start of time interval. (*A*) Net reduction of inflammation (calprotectin level), no change of microbiota state. (*B*) Net reduction of inflammation, change of microbiota state. (*C*) Net increase of inflammation, no change of microbiota state. (*D*) Net increase of inflammation, no change of microbiota state. (*E*) Trajectories of 4 selected patients; see main text for explanation. (*F*) Trajectories of 4 selected patients; see main text for explanation.

representing microbiota state change (Figure 3*D*) part from the upper left corner of the plot and globally point to the lower right corner. This behavior appears coherent with the overall correlation between an increase of inflammation and a deterioration of the microbiota (Figure 1*F*), and it may seem to support the hypothesis that no alternative state barriers exist (even if several of these vectors point steeper downward than might be expected). It can also be explained in an alternative states context, however. Several vectors in Figure 3*C* and *D* indicate that inflammation may surge to high levels, approaching the tipping point between microbiota states M4 and M3 (at approximately 5000 μg calprotectin/g; see section on "Four Alternative Microbiota States"). Inflammation may even have reached still higher levels and subsequently been compensated to a greater or lesser extent, considering that the vectors represent net changes between 2 timepoints and not the actual patient trajectories. The downward-pointing vectors may thus represent patients who reached a tipping point at a high inflammation level; made a downward microbiota state transition (Figure 1*J*); and, within the new microbiota state, were pushed back to a lower inflammation level. The trajectories of several patients support this possibility on the timescale from T4 to T52 (48 weeks) (Figure 3*E*), whereas nearly all the vectors concerned in Figure 3*D* represent the interval of T12–T52 (40 weeks).

Crucially, a second group of vectors points upward from the lower left corner of Figure 3*D*, combining a strong increase in inflammation with a microbiota change toward the healthier M4 state. These vectors contradict a linear microbiota-host relationship model, where changes would take place along a diagonal from the top left to bottom right (Figure 1*F*) but can be explained in the context of the alternative stable states model. The actual trajectory of these patients could have passed through a low inflammation level and a concomitant transition to a higher microbiota state before being pushed to a higher inflammation level within the new microbiota state. This possibility is supported by the trajectories of several patients over a period of 12 or 52 weeks (Figure 3*F*).

The different categories of observations in Figure 3*C* and *D* thus are consistent with the alternative microbiota states model and supported by observed patient trajectories over similar time intervals, even if more frequent sampling would have been necessary to document actual patient trajectories within single time-step intervals. Only 1 of the 3 categories of vectors appears compatible with a model without involvement of alternative microbiota states.

Evolution of Host Inflammatory Status

The evolution of host status cannot be evaluated in the same way as that of microbiota status, because this would need microbiota-directed intervention while letting inflammation freely evolve. Nonetheless, the evolution of the inflammation component is telling. Under net anti-inflammatory or net inflammatory pressure, similar patterns are observed (Figure 4*A* and *B*): although over a given time interval patients can be (actively) pushed over inflammation state boundaries, they often remain in the same state or end up in the adjacent state. In either direction, the overall picture gives an impression of pausing in progression on the inflammation scale, with an accumulation of patients in the earlier defined alternative states (Figure 4*A* and *B*: positions of arrowheads). This picture is in stark contrast to the random distribution that might be expected in the absence of alternative host states, especially given the large diversity in inflammatory status among patients at T0 (Figure 2*D*) and the diversity in the lengths of the time intervals considered (4, 8, or 40 weeks). The same patterns are observed when only the first treatment interval is considered (T0–T4) (Supplementary Figure 9*A* and *B*), independent of treatment. Under anti-inflammatory pressure, a similar pattern of pausing at host states H3 or H2 is observed when selecting patients for whom host state H1 has proven accessible (ie, with at least 1 timepoint showing host state H1) (Supplementary Figure 9*C*).

Together, the longitudinal data strongly suggest that alternative host and microbiota states affect treatment success. This is reflected in a retardation of progression to a healthier state of the ecosystem, with pausing or even blockage at intermediate, less favorable states. Under current treatment practice, which focuses on the suppression of inflammation and eliminates much of the initial difference among patients regarding this parameter, it appears that initial microbiota state remains a discriminating element of treatment success if not actively acted on: remission at T52, 1 year after the start of treatments, depends on the microbiota state before treatment (at T0) (Figure 4*C*). At the same time, alternative states are also expected to retard decline, making the progression of disease a stepwise process. The analysis of time intervals with a net increase of inflammation confirms this prediction.

Discussion

Current clinical practice in the treatment of UC focuses on the suppression of inflammation. Success rates are low, and relapse is common. We recently proposed that alternative stable states of the intestinal ecosystem and their expected behavior could be part of the problem and, when understood, of the solution.[1,2] We showed that alternative intestinal microbiota and host states can be detected under controlled conditions in a rat model[2] and showed that the existence of these alternative states could also be documented using the intrinsic properties of the ecosystem, analyzing the microbiota component as a function of the host component and vice versa. This suggested that alternative states of the intestinal ecosystem could also be studied when external conditions are not strictly controlled or controllable, which would present 2 major advantages for the study of the human intestinal ecosystem: (1) strict control of external conditions, extremely difficult to achieve over a long period of time for an important number of patients, would not be necessary, and consequently, (2) this approach would permit the

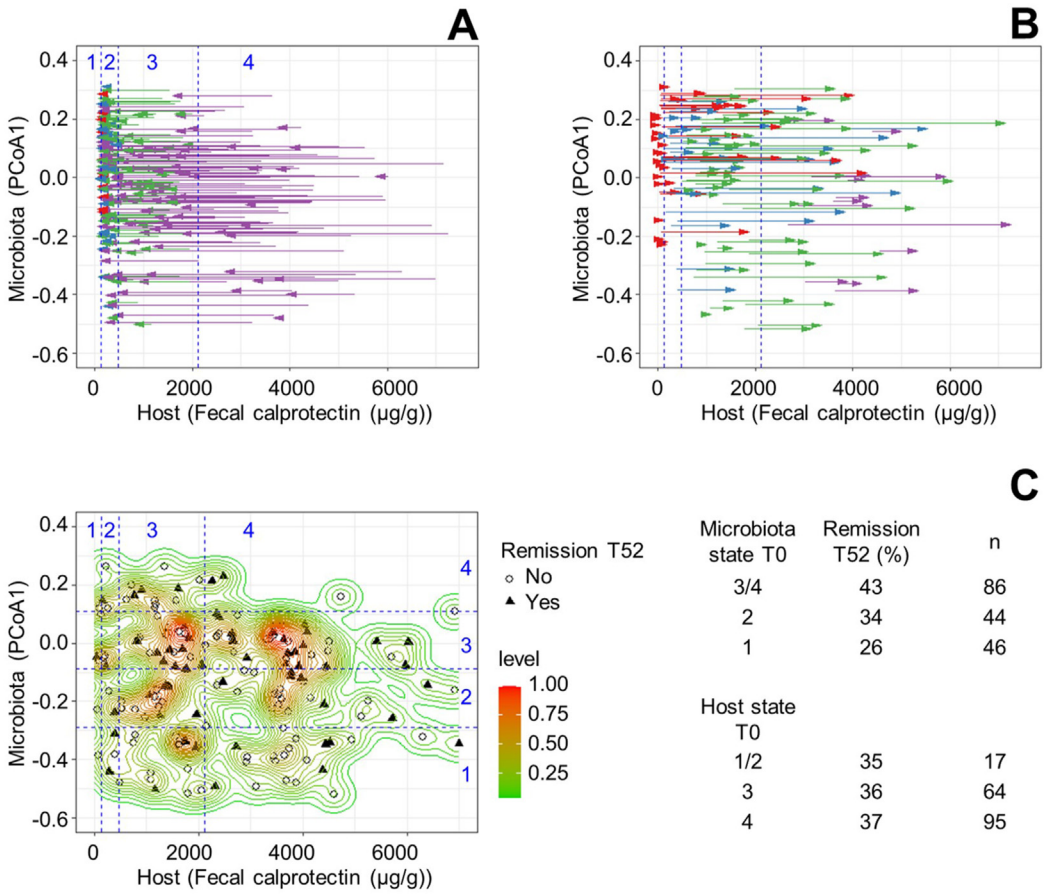

Figure 4. Evolution of host inflammatory status. (*A*, *B*) Vectors indicate the evolution of the inflammation status (fecal calprotectin) of a given patient from one timepoint to the next (T0 to T4, T4 to T12, or T12 to T52). Alternative host states as in Figure 2*A*. Patients who had used antibiotics within a period of 27 days before stool sample collection were excluded. Colors indicate host state at start of time interval. (*A*) Net reduction of inflammation (calprotectin level). (*B*) Net increase of inflammation. (*C*) As in Figure 2*C*. Only data from treatment-naive patients (T0) for whom remission was evaluated at T52 are shown. Symbols, remission or not at T52, as indicated. Table shows percentages of patients in remission at T52 as a function of microbiota or host state at T0. Percent remission at T52 increases from T0 microbiota state 1 to 3/4 ($P = .03$, chi-square trend test) but is independent of T0 host state 1/2 to 4 ($P = .88$).

analysis of data coming directly from real-life clinical practice to render results that are highly relevant for potential adjustments in clinical management.

In this study, we apply this approach to earlier published data collected during the treatment of pediatric patients with UC.[6] We identify 4 alternative microbiota states and 4 alternative host states. At least 3 of each were also observed in treatment-naive patients, indicating that the alternative states are not created by the anti-inflammatory treatments. Rather, treatments redistribute individuals over possible ecosystem states.

Our present view is that multiple alternative states, not limited to the states we identify here, may exist as possible stable configurations of the intestinal ecosystem. External factors, among which are long-term diet or lifestyle factors, may determine the larger contours and shape of this landscape of possible states (and cause or prevent state transitions themselves[1]). Other factors (for example, specific disease–inducing factors) may influence the distribution of individuals over the landscape of possible states and shape local landscape detail. Although this view is not unlike what has been proposed by others, here, we provide the first experimental evidence to our knowledge for the existence of alternative states of the human intestinal ecosystem. Our study takes both the microbiota and the host component of the system into account, thereby extending on an earlier microbiota-only exploration that resulted in the definition of *tipping elements* rather than alternative ecosystem states.[15]

The alternative states described in this study are those that are relevant in the context of (pediatric) UC. Do they influence treatment efficacy? The longitudinal data strongly suggest that they do. They support the alternative states model of the intestinal ecosystem and provide strong indications that alternative state properties delay or prevent remission from UC under an anti-inflammatory treatment protocol.

Although standard-of-care anti-inflammatory treatments appear to be efficient to overcome at least some of the hurdles of alternative host inflammatory states, only 36% of patients (30% of patients in remission at T52) reached a nonpathologic inflammation level. Remaining (low-level)

inflammation, if going unnoticed in disease assessment, may be a cause of future relapse through the initiation of a vicious cycle of deleterious host-microbiota interactions.[1] The restoration of a healthy microbiota remains a critical factor on the way to remission, as illustrated by the observation that 1 year after the start of treatments, remission proves to depend on the microbiota state before treatment. These observations suggest that active microbiota management, in combination with anti-inflammatory treatments, could improve treatment success. The theory of alternative intestinal ecosystem states points in the same direction. Some of the important microbiota tipping points are inaccessible at negative inflammation values (calprotectin levels) (Figure 1*J*), preventing a systematic restoration of a healthy microbiota through mere inflammation suppression. Transitions to a low inflammation state could be facilitated by a favorable microbiota (Figure 1*M*). Combined action on both the host and microbiota is predicted to require less effort on each of these parameters to ensure transition to a healthy state, without the need to reach the respective tipping points, than action on only 1 parameter in a model where all tipping points are accessible.[2] In (pediatric) UC, where some of the tipping points in the reconstitution of a healthy intestinal ecosystem prove inaccessible, a concerted action on inflammation and microbiota becomes crucial to ensure remission (compare with the Graphical Abstract).

The present model, based on intrinsic properties of the intestinal ecosystem (host inflammation level and microbiota composition), and its recommendations cannot be seen as disconnected from the environment, which we, as stated, think is pivotal in determining the larger contours of the landscape of possible alternative states. For example, long-term diet is known to have a profound effect on microbiota composition and diversity,[16,17] and therefore a healthy microbiota (generally associated with high diversity[14]) might be out of reach if not sustained by dietary habits. In this study, a major obstacle appears to block the transition to microbiota state M4, even when inflammation is reduced to close to 0 (Figure 1*I*). It seems unlikely that, in this case, blockage would be due to a general factor such as the Western diet in some of the patients, because OTU richness is comparable in microbiota states M3 and M4 (Table 2). However, we cannot exclude that a more specific unidentified diet, lifestyle, or other factor (UC is a multifactorial disease) could deny access to microbiota state M4 for some patients. Even in that case, the dependency of transition on inflammation level remains for those patients who can reach microbiota state M4. This consideration, therefore, does not contradict the interfering role of alternative microbiota states in the reconstitution of a healthy microbiota. It does suggest, however, that still other levers than inflammation reduction and microbiota management may have to be actioned to sustain durable remission.

The discovery of alternative stable microbiota and host states allows an enhanced understanding of the evolution of a patient's clinical pictures under treatment, taking intestinal microbiota and inflammation status into account, and may explain why some patients do not respond to anti-inflammatory treatment or FMT as we would like. A recent commentary calling for the development of combination therapies to overcome the plateau of drug efficacy in inflammatory bowel diseases suggested that targeting inflammation and microbiota might be one of the most promising future avenues.[4] Our model of alternative intestinal ecosystem states provides a strong rationale for these combination therapies and can be used as a framework to monitor and direct disease treatment.

Supplementary Material

Note: To access the supplementary material accompanying this article, visit the online version of *Gastroenterology* at www.gastrojournal.org, and at https://doi.org/10.1053/j.gastro.2021.08.057.

References

1. Van de Guchte M, Blottiere HM, Dore J. Humans as holobionts: implications for prevention and therapy. Microbiome 2018;6(1):81.
2. **Van de Guchte M, Burz SD**, Cadiou J, et al. Alternative stable states in the intestinal ecosystem: proof of concept in a rat model and a perspective of therapeutic implications. Microbiome 2020;8(1):153.
3. Scheffer M, Carpenter S, Foley JA, et al. Catastrophic shifts in ecosystems. Nature 2001;413(6856):591–596.
4. Stalgis C, Deepak P, Mehandru S, et al. Rational combination therapy to overcome the plateau of drug efficacy in inflammatory bowel disease. Gastroenterology 2021;161:394–399.
5. Martin JC, Bériou G, Josien R. Dextran sulfate sodium (DSS)-induced acute colitis in the rat. Methods Mol Biol 2016;1371:197–203.
6. Schirmer M, Denson L, Vlamakis H, et al. Compositional and temporal changes in the gut microbiome of pediatric ulcerative colitis patients are linked to disease course. Cell Host Microbe 2018;24:600–610.
7. Turner D, Otley AR, Mack D, et al. Development, validation, and evaluation of a pediatric ulcerative colitis activity index: a prospective multicenter study. Gastroenterology 2007;133:423–432.
8. Ma R, Meng R, Zhang X, et al. Correlation between fecal calprotectin, ulcerative colitis endoscopic index of severity and clinical outcome in patients with acute severe colitis. Exp Ther Med 2020;20:1498–1504.
9. Kawashima K, Ishihara S, Yuki T, et al. Fecal calprotectin level correlated with both endoscopic severity and disease extent in ulcerative colitis. BMC Gastroenterol 2016;16:47.
10. D'Amico F, Bonovas S, Danese S, et al. Review article: faecal calprotectin and histologic remission in ulcerative colitis. Aliment Pharmacol Ther 2020;51:689–698.
11. Haifer C, Leong RW, Paramsothy S. The role of faecal microbiota transplantation in the treatment of

inflammatory bowel disease. Curr Opin Pharmacol 2020;55:8–16.
12. Costello SP, Soo W, Bryant RV, et al. Systematic review with meta-analysis: faecal microbiota transplantation for the induction of remission for active ulcerative colitis. Aliment Pharmacol Ther 2017;46:213–224.
13. Yatsunenko T, Rey FE, Manary MJ, et al. Human gut microbiome viewed across age and geography. Nature 2012;486(7402):222–227.
14. **Le Chatelier E, Nielsen T, Qin J, Prifti E**, et al. Richness of human gut microbiome correlates with metabolic markers. Nature 2013;500(7464):541–546.
15. Lahti L, Salojärvi J, Salonen A, et al. Tipping elements in the human intestinal ecosystem. Nat Commun 2014; 5:4344.
16. **Smits SA, Leach J**, Sonnenburg ED, et al. Seasonal cycling in the gut microbiome of the Hadza hunter-gatherers of Tanzania. Science 2017;357(6353):802–806.
17. Wu GD, Chen J, Hoffmann C, et al. Linking long-term dietary patterns with gut microbial enterotypes. Science 2011;334(6052):105–108.
18. Scrucca L, Fop M, Murphy TB, et al. mclust 5: clustering, classification and density estimation using Gaussian finite mixture models. R J 2016;8:289–317.
19. **Qin J, Li R**, Raes J, et al. A human gut microbial gene catalogue established by metagenomic sequencing. Nature 2010;464(7285):59–65.
20. **Arumugam M, Raes J**, Pelletier E, et al. Enterotypes of the human gut microbiome. Nature 2011;473(7346):174–180.
21. Costea PI, Hildebrand F, Manimozhiyan A, et al. Enterotypes in the landscape of gut microbial community composition. Nat Microbiol 2018;3:8–16.
22. Manichanh C, Rigottier-Gois L, Bonnaud E, et al. Reduced diversity of faecal microbiota in Crohn's disease revealed by a metagenomic approach. Gut 2006; 55:205–211.

Author names in bold designate shared co-first authorship.

Received June 7, 2021. Accepted August 29, 2021.

Correspondence
Address correspondence to: Maarten van de Guchte, PhD, INRAE, Micalis Institute, Domaine de Vilvert, 78350 Jouy-en-Josas, France. e-mail: maarten.van-de-guchte@inrae.fr.

CRediT Authorship Contributions
Maarten Van de Guchte, PhD (Conceptualization: Equal; Formal analysis: Lead; Investigation: Lead; Methodology: Lead; Visualization: Lead; Writing – original draft: Lead; Writing – review & editing: Lead); Stanislas Mondot, PhD (Formal analysis: Equal; Methodology: Equal; Visualization: Supporting); Joël Doré, PhD (Conceptualization: Equal; Funding acquisition: Lead; Writing – review & editing: Supporting).

Conflicts of interest
The authors disclose no conflicts.

Funding
This project was funded by the European Commission under ERC-2017-AdG n. 788191 - Homo.symbiosus.

Supplementary References

e1. Scrucca L, Fop M, Murphy TB, et al. mclust 5: clustering, classification and density estimation using Gaussian finite mixture models. R J 2016;8:289–317.

e2. Schirmer M, Denson L, Vlamakis H, et al. Compositional and temporal changes in the gut microbiome of pediatric ulcerative colitis patients are linked to disease course. Cell Host Microbe 2018;24:600–610.

e3. Yatsunenko T, Rey FE, Manary MJ, et al. Human gut microbiome viewed across age and geography. Nature 2012;486(7402):222–227.

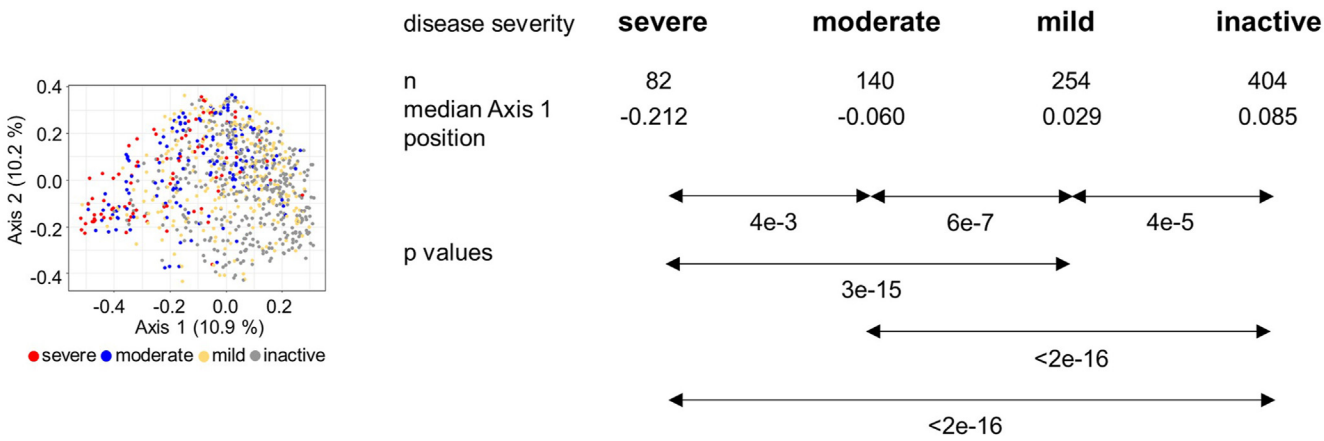

Supplementary Figure 1. Microbiota and disease severity classes. PCoA of ecological distances between microbiota samples (compare with Figure 1*E*). Colors indicate disease severity classes. *P* values indicate the probability that 2 disease severity classes represent the same patient distribution (Kruskal-Wallis rank-sum test with Dunn post hoc test and Bonferroni adjustment for multiple comparisons).

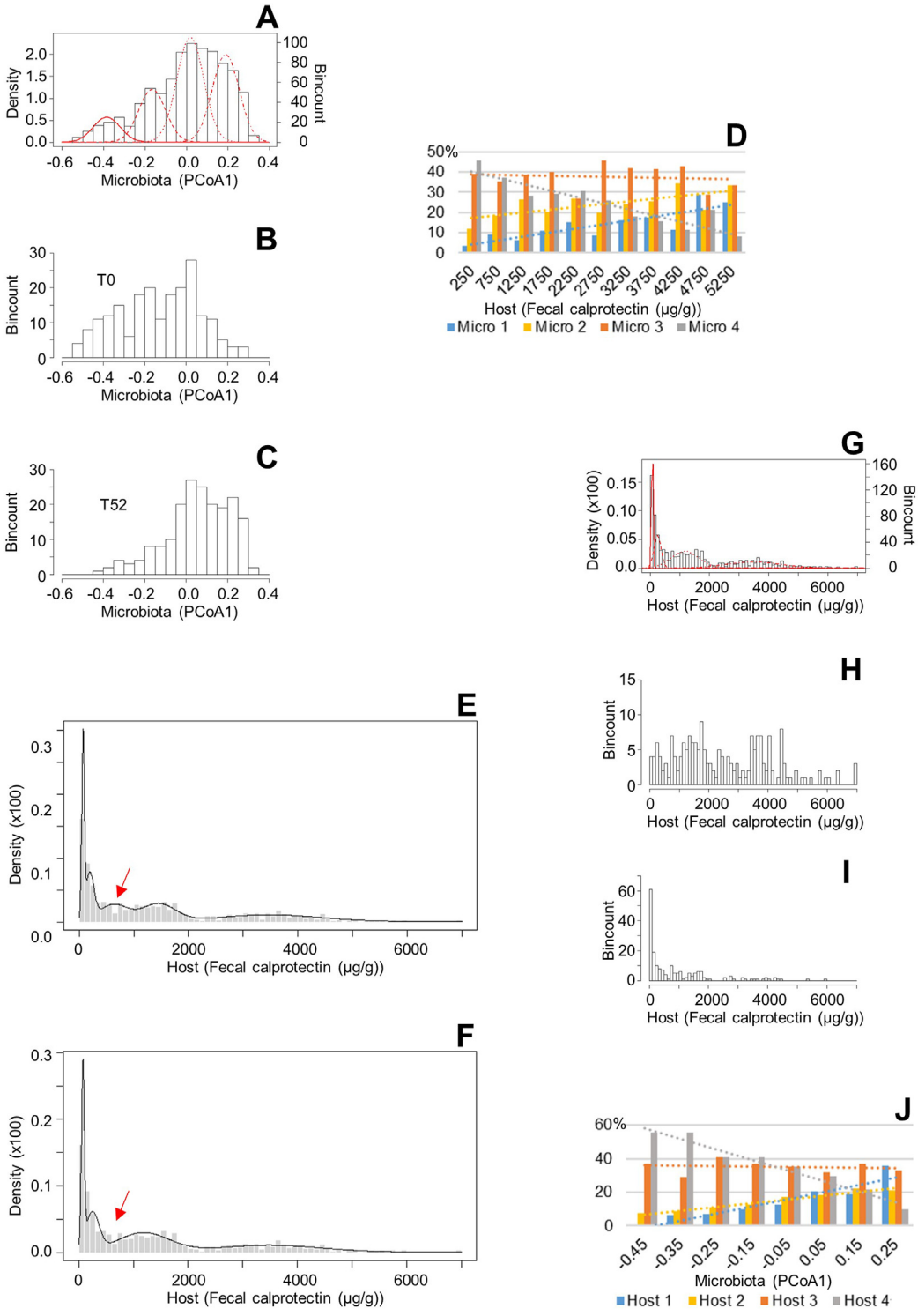
A
Density
Bincount
Microbiota (PCoA1)
B
T0
Bincount
Microbiota (PCoA1)
C
T52
Bincount
Microbiota (PCoA1)
D
Host (Fecal calprotectin (µg/g))
Micro 1
Micro 2
Micro 3
Micro 4
E
Density (x100)
Host (Fecal calprotectin (µg/g))
F
Density (x100)
Host (Fecal calprotectin (µg/g))
G
Density (x100)
Bincount
Host (Fecal calprotectin (µg/g))
H
Bincount
Host (Fecal calprotectin (µg/g))
I
Bincount
Host (Fecal calprotectin (µg/g))
J
Microbiota (PCoA1)
Host 1
Host 2
Host 3
Host 4

Supplementary Figure 2. Multimodal distributions of microbiota and host status. (*A–C*) PCoA1 coordinates from the ordination plot in Figure 1*E* as a measure of microbiota status are divided in categories with a range of 0.05, and the frequency of occurrence of each category is plotted. (*A*) All data (compare with Figure 1*H*). (*B*) Data from T0 only (ie, before anti-inflammatory treatment). (*C*) Data from T52 only (ie, after anti-inflammatory treatment). (*D*) Correlations between relative frequencies of alternative microbiota states and host inflammatory status. Host inflammatory status by fecal calprotectin levels are binned in intervals of 500 μg/g; the central value of each bin is indicated. Bins with calprotectin levels of >5500 μg/g contained fewer than 10 observations per bin (compare with Figure 1*I*) and are ignored. Linear regression of microbiota state M1 vs host status: $r^2 = 0.71$; $p = .001$ (*F* test); microbiota state M2: $r^2 = 0.48$; $P = .019$; microbiota state M3: $r^2 = 0.01$; $P = .734$; microbiota state M4: $r^2 = 0.84$; $P = 6.6e{-}5$. (*E–I*) Fecal calprotectin levels as a measure of host inflammatory status are divided in categories with a range of 100 μg/g, and the frequency of occurrence of each category is plotted. (*E*) Density graph overlays according to the results of finite Gaussian mixture modeling using mclust 5.4,[e1] with 6 components. (*F*) As in *E*, with 5 components. Mclust initially fits a model with 6 components based on the maximal value of the Bayesian information criterion (BIC) (–14,647). A model with 5 components obtained essentially the same BIC value (–14,656). The maximal value of a different criterion, the integrated classification likelihood criterion, points at a model with 5 components. Based on these results, we decided to use the model with 5 components rather than 6 as a basis for simplicity and because this model appears to give a better fit in the calprotectin range from 400 to 1,000 μg/g (compare *E* and *F*). In practice, the 5 components are then treated as 4 components, because the fifth component (with an estimated mean and SD of 6850 $\pm$ 3183) contains only 28 very dispersed observations (ie, only 3% of the 881 observations), making it far from sure that these should be considered as a separate host state. (*G*) As in *E*, with 4 components (compare with Figure 1*K*). (*H*) Data from T0 only. (*I*) Data from T52 only. (*J*) Correlations between relative frequencies of alternative host states and microbiota status. Microbiota status, PCoA1 values (Figure 1*E*) are binned in intervals of 0.1; the central value of each bin is indicated. Bins with PCoA1 values of <–0.5 or >0.3 contained fewer than 10 observations per bin (compare with Figure 1*L*) and are ignored. Linear regression of host state H1 vs microbiota status: $r^2 = 0.87$; $P = 7.6e{-}4$ (*F* test); host state H2: $r^2 = 0.96$; $P = 1.7e{-}5$; host state H3: $r^2 = 0.02$; $P = .734$; host state H4: $r^2 = 0.96$; $P = 2.7e{-}5$.

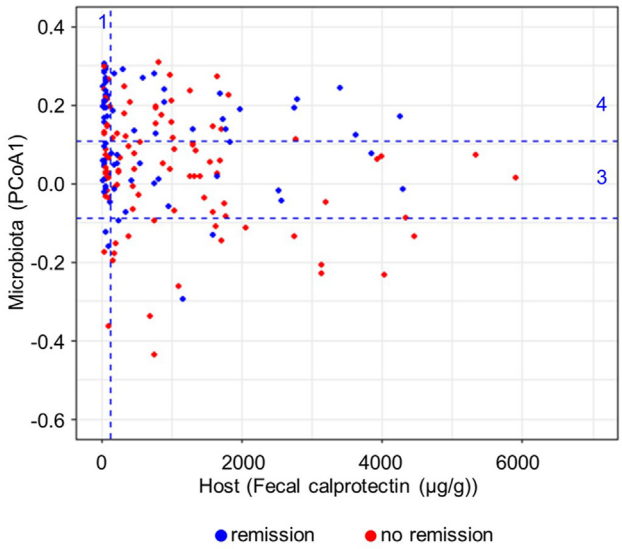

Supplementary Figure 3. Microbiota state and remission. Microbiota status (position on the PCoA1 axis from Figure 1*E*) vs host inflammatory status (fecal calprotectin level) at T52. Numbers 3 and 4 indicate alternative microbiota states (Figure 1*H*). Number 1 indicates host state 1 (Figure 1*K*). Patients who had used antibiotics within a period of 27 days before stool sample collection were excluded. Colors show remission (defined as having a Pediatric UC Activity Index score of <10 and not being on corticosteroid therapy for a minimum of 28 days before the assessment time[e2]) or not at T52, as indicated. Overall, 56% of patients with microbiota state 4 were in remission vs 38% of patients with microbiota state 3 ($P = .025$, 2-sided Fisher exact test; no significant difference in inflammation was observed between the 2 microbiota states at T52). The same tendency is visible among patients with host state 1 (inflammation close to 0): 68% of patients with microbiota state 4 were in remission vs 48% of patients with microbiota state 3 ($P = .19$; not significant because of the lower number of observations).

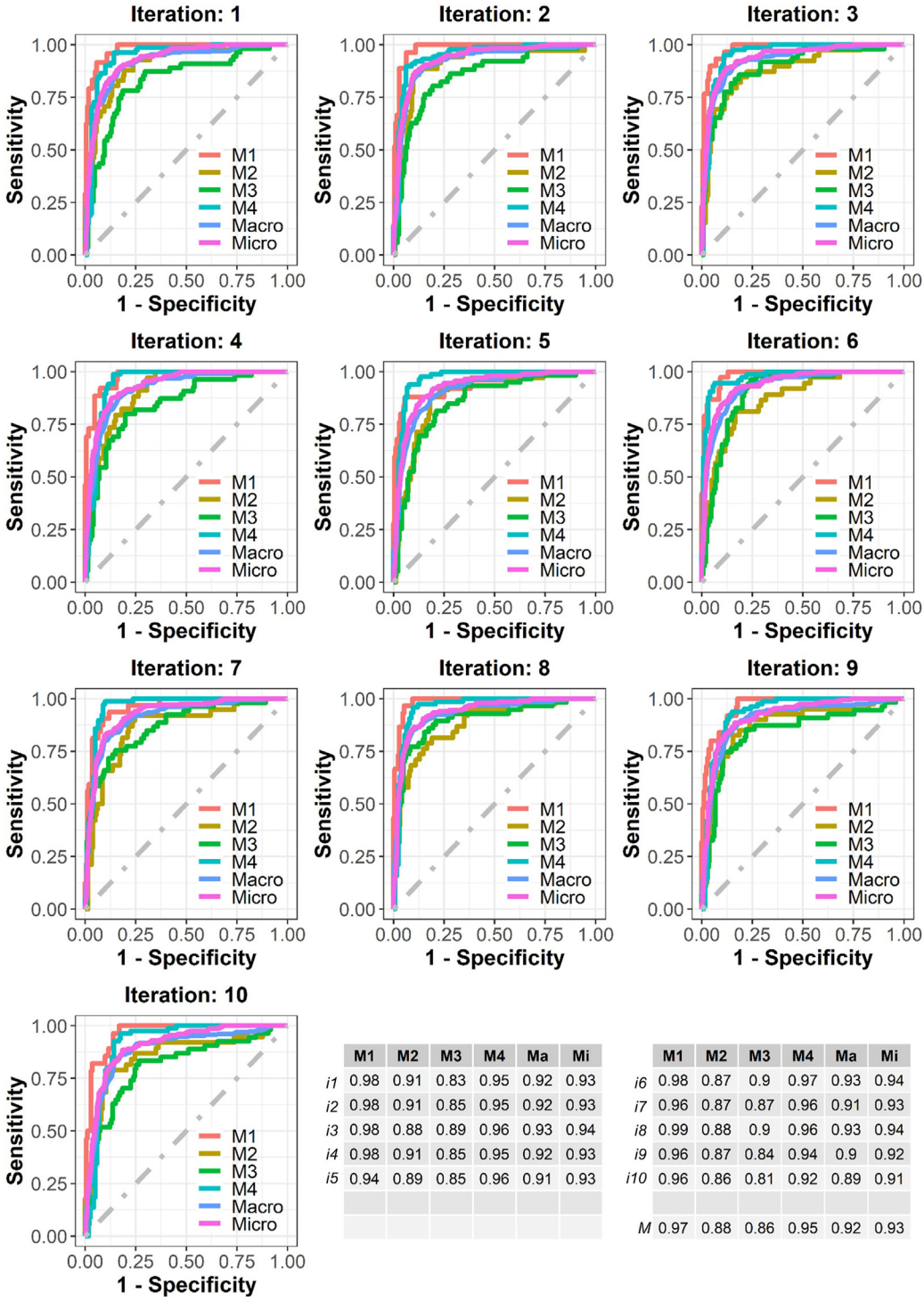

	M1	M2	M3	M4	Ma	Mi
i1	0.98	0.91	0.83	0.95	0.92	0.93
i2	0.98	0.91	0.85	0.95	0.92	0.93
i3	0.98	0.88	0.89	0.96	0.93	0.94
i4	0.98	0.91	0.85	0.95	0.92	0.93
i5	0.94	0.89	0.85	0.96	0.91	0.93

	M1	M2	M3	M4	Ma	Mi
i6	0.98	0.87	0.9	0.97	0.93	0.94
i7	0.96	0.87	0.87	0.96	0.91	0.93
i8	0.99	0.88	0.9	0.96	0.93	0.94
i9	0.96	0.87	0.84	0.94	0.9	0.92
i10	0.96	0.86	0.81	0.92	0.89	0.91
M	0.97	0.88	0.86	0.95	0.92	0.93

Supplementary Figure 4. Receiver operating characteristics (ROCs) of microbiota classification models (I). The 17 differentially abundant genera from Table 1 were used to develop multiclass area under the curve (AUC) models that classify microbiota samples as belonging to microbiota state M1, M2, M3m or M4. Ten training sets of 201 randomly picked microbiota samples from Table 1 were constituted, each with the same proportions of M1, M2, M3, and M4 samples as in the full data set (402 samples), using the R package caret. Multinomial log-linear models were generated using the R package nnet. Graphs show the results of "one (M1, M2, M3 or M4) vs rest" ROC analyses of the classification models on the remaining 201 samples using the R package multiROC. The table gives AUC values for each class for each iteration and the averages (M) per class. Ma, macroaverage; Macro, macroaverage; Mi, microaverage; Micro, microaverage.

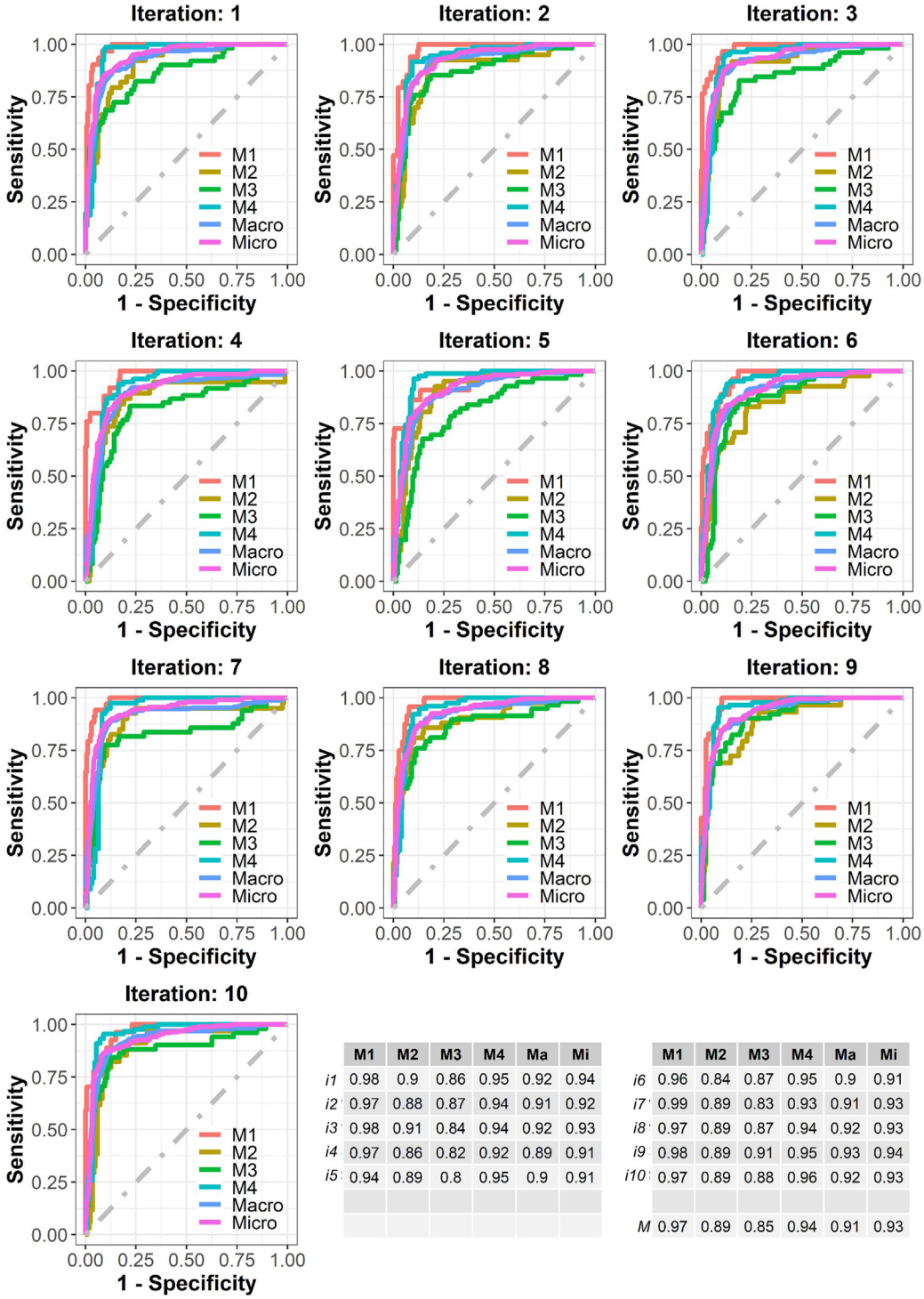

	M1	M2	M3	M4	Ma	Mi
i1	0.98	0.9	0.86	0.95	0.92	0.94
i2	0.97	0.88	0.87	0.94	0.91	0.92
i3	0.98	0.91	0.84	0.94	0.92	0.93
i4	0.97	0.86	0.82	0.92	0.89	0.91
i5	0.94	0.89	0.8	0.95	0.9	0.91

	M1	M2	M3	M4	Ma	Mi
i6	0.96	0.84	0.87	0.95	0.9	0.91
i7	0.99	0.89	0.83	0.93	0.91	0.93
i8	0.97	0.89	0.87	0.94	0.92	0.93
i9	0.98	0.89	0.91	0.95	0.93	0.94
i10	0.97	0.89	0.88	0.96	0.92	0.93
M	0.97	0.89	0.85	0.94	0.91	0.93

Supplementary Figure 5. ROCs of microbiota classification models (II). As in Supplementary Figure 4, 14 of the differentially abundant genera were used (ie, excluding the genera *Eikenella*, *Aggregatibacter*, and *Erwinia* [see Supplementary Figure 6]).

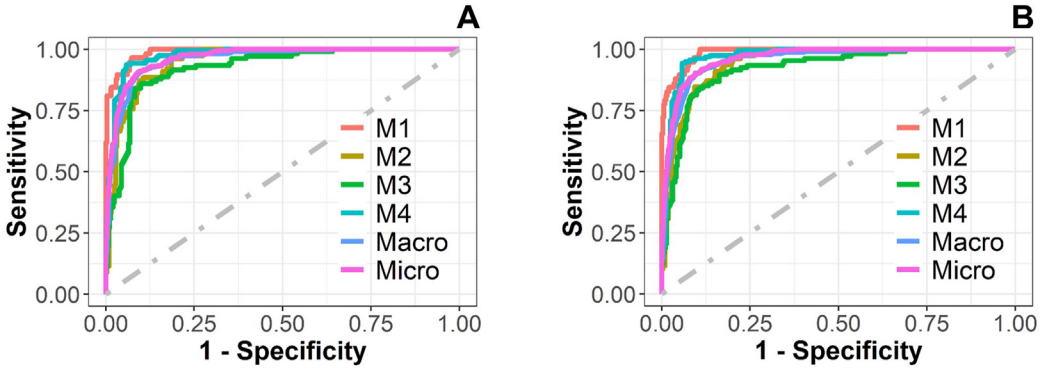

	M1	M2	M3	M4	Ma	Mi
AUC	0.99	0.95	0.93	0.97	0.96	0.97

	M1	M2	M3	M4	Ma	Mi
AUC	0.99	0.95	0.92	0.97	0.96	0.96

C

Microbiota state	M1	M2	M3	M4
n	0	1*	1**	252

*male, age 50, BMI 38
**female, age 46, BMI 21

Supplementary Figure 6. ROCs of microbiota classification models (III). (*A*) ROC analysis of a model generated using the 17 genera from Table 1 and all 402 microbiota samples as the training set, with validation on the same data set. (*B*) As in *A*, using 14 of the differentially abundant genera (ie, excluding the genera *Eikenella*, *Aggregatibacter*, and *Erwinia*). (*C*) The model obtained under *B* was used to classify microbiota samples from 254 healthy US citizens (125 aged 4–17 years, 129 aged 18–58 years), in which the genera *Eikenella*, *Aggregatibacter*, and *Erwinia* were absent.[e3] BMI, body mass index.

A

T0 (%, n = 185)

microbiota states \ host states	1	2	3	4	total
4	0.5	1.6	5.9	1.6	9.7
3	1.1	2.2	13.0	23.8	40.0
2	0.5	1.1	9.2	14.1	24.9
1	0.5	1.6	9.2	14.1	25.4
total	2.7	6.5	37.3	53.5	100

T4 (%, n = 212)

microbiota states \ host states	1	2	3	4	total
4	7.1	11.8	16.0	3.3	38.2
3	4.7	8.5	14.2	9.4	36.8
2	2.4	3.8	7.5	5.2	18.9
1	0.0	0.5	1.9	3.8	6.1
total	14.2	24.5	39.6	21.7	100

T12 (%, n = 230)

microbiota states \ host states	1	2	3	4	total
4	14.8	8.3	11.7	7.4	42.2
3	9.6	6.5	12.6	12.6	41.3
2	1.7	2.2	5.7	5.2	14.8
1	0.0	0.0	0.4	1.3	1.7
total	26.1	17.0	30.4	26.5	100

T52 (%, n = 178)

microbiota states \ host states	1	2	3	4	total
4	19.1	5.6	13.5	3.9	42.1
3	14.6	10.1	14.6	5.6	44.9
2	1.7	2.8	3.4	2.8	10.7
1	0.6	0.0	1.7	0.0	2.2
total	36.0	18.5	33.1	12.4	100

B

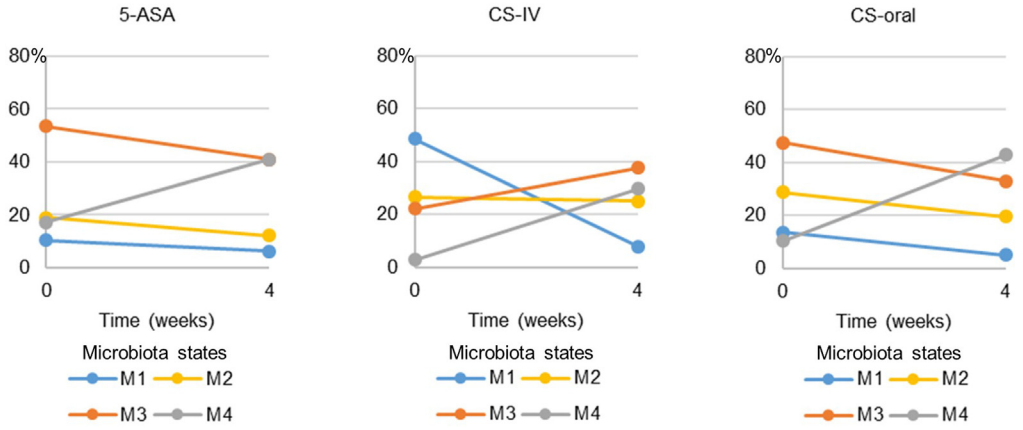

Supplementary Figure 7. Microbiota and host states at different timepoints. (*A*) Distribution of patients over alternative host and microbiota states at 4 sampling timepoints. Data from Figure 2*D*. Observations are attributed to different host and microbiota states based on models generated by mclust (Figure 1*H* and *K*). State distributions are partially overlapping, meaning that for a given observation, the probability of belonging to a given state is >50%. Patients who had used antibiotics within a period of 27 days before stool sample collection were excluded. Not all patients are represented at all timepoints; see Scrucca et al[e1] for details (a total of 805 observations for 353 patients). (*B*) Relative abundance of different host states before (T0) and after (T4) different treatments. 5-ASA, mesalamine; CS-IV, intravenous steroids; CS-oral, oral steroids.

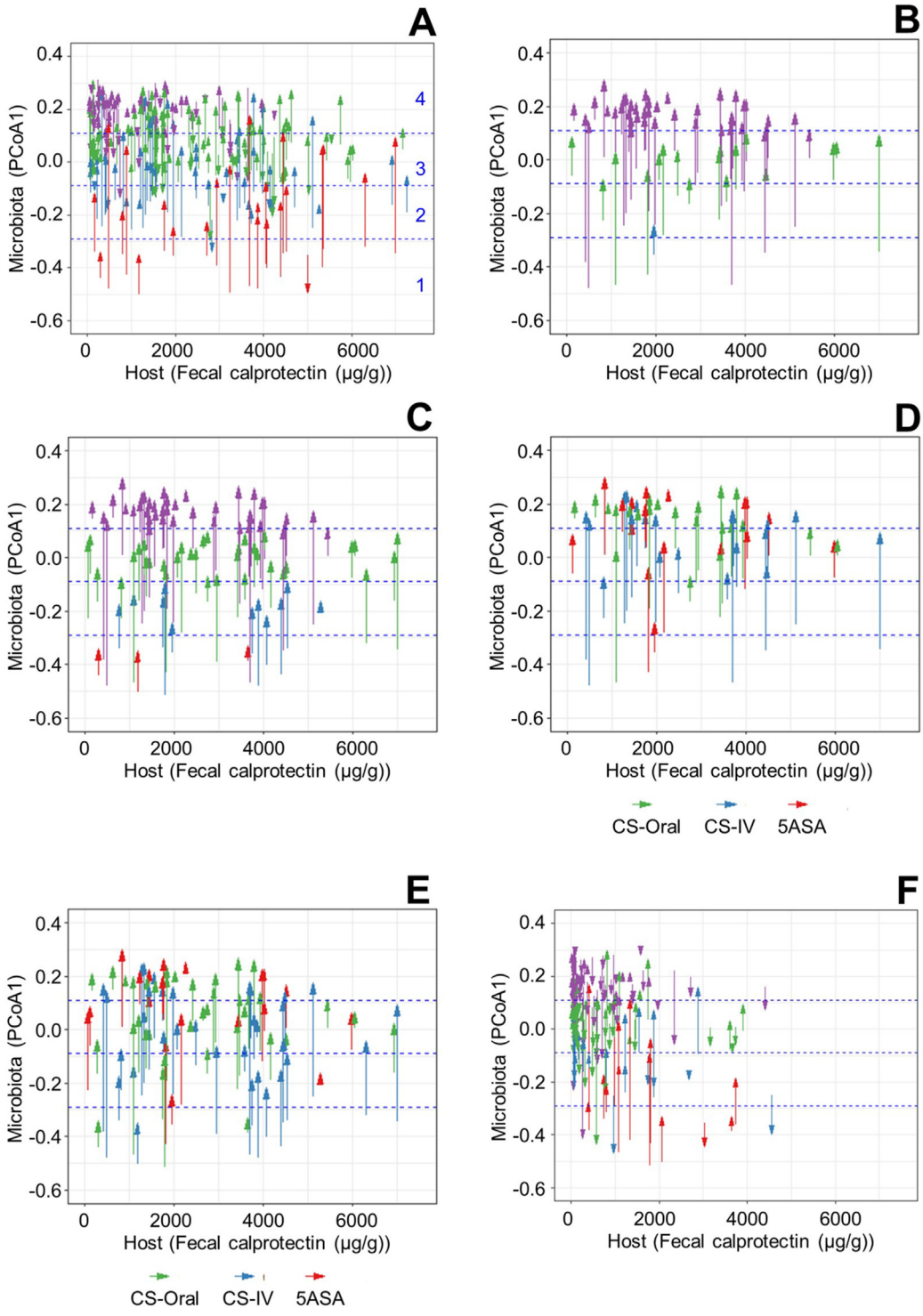

Supplementary Figure 8. Evolution of microbiota status. (*A*) Arrows indicate the evolution of the microbiota component of the intestinal ecosystem of a given patient from one timepoint to the next (T0 to T4, T4 to T12, or T12 to T52) for patients showing a net reduction of inflammation. Colors indicate microbiota state at the start of the time interval. (*B*) As in *A*, for patients showing a net increase of microbiota PCoA1 and for whom microbiota state M4 has proven accessible (at least 1 observation in microbiota state M4). T0 to T4 only, colors indicate microbiota state at T4. (*C*) As in *B*, for patients for whom at least microbiota state M3 has proven accessible. (*D*) As in *B*; colors indicate treatment. (*E*) As in *C*; colors indicate treatment. (*F*) As in *A*, for patients showing a net increase of inflammation. All panels: patients who had used antibiotics within a period of 27 days before stool sample collection were excluded. Numbers 1–4 indicate alternative microbiota states (Figure 1*H*).

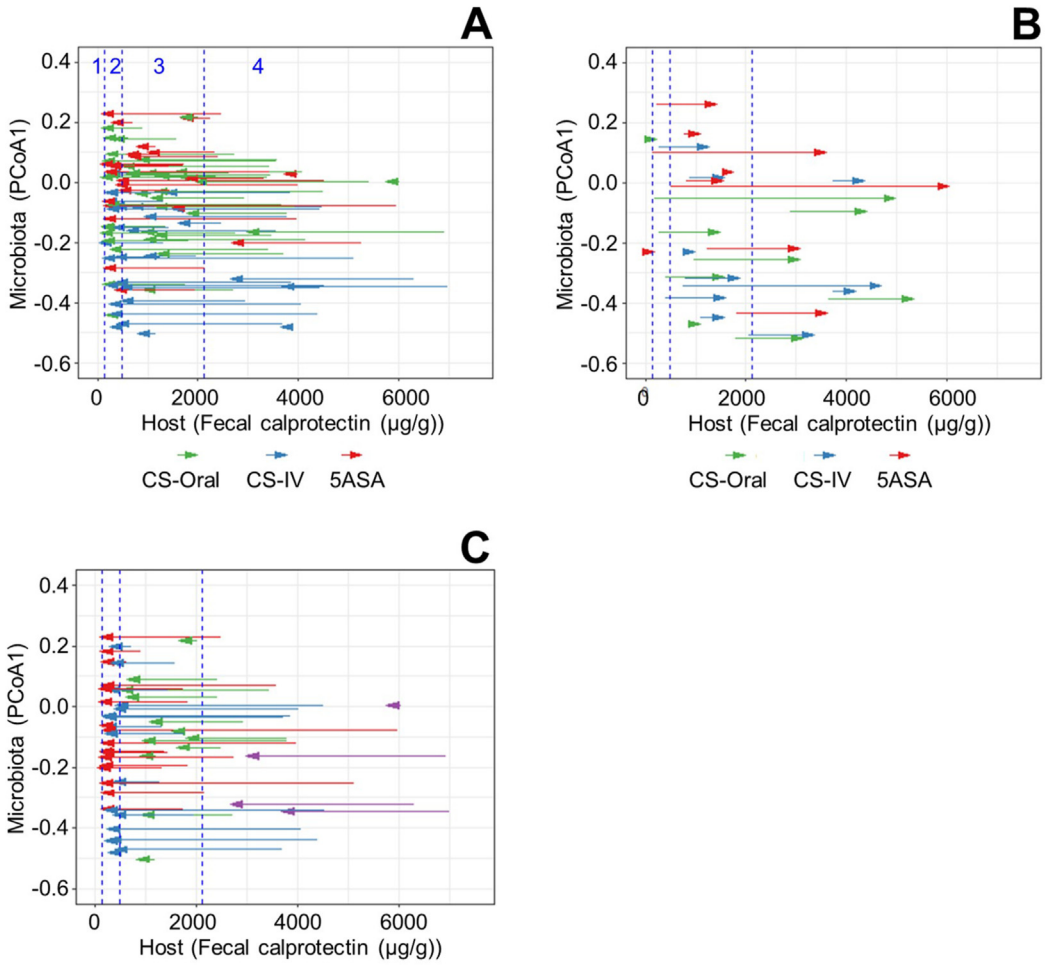

Supplementary Figure 9. Evolution of host status. (*A*) Arrows indicate the evolution of the host component of the intestinal ecosystem of a given patient from T0 to T4 for patients showing a net reduction of inflammation. Colors indicate treatment during this time interval. (*B*) As in *A*, for patients showing a net increase of inflammation. (*C*) As in *A*, for patients for whom host state H1 has proven accessible (at least 1 observation in host state H1). Colors indicate host state at T4. All panels: patients who had used antibiotics within a period of 27 days before stool sample collection were excluded. Numbers 1–4 indicate alternative host states (Figure 1*K*).

Supplementary Table 1. Microbiota PCoA1 Distribution in Groups of Specified Host Fecal Calprotectin Range

Calprotectin range, $\mu g/g$	Observations, n	Shapiro test for normality, *P*	mclust BIC components, n	mclust LRT components, n	LRT bootstrap, *P*	Mean PCoA1 values for components, based on n by LRT			
						1	2	3	4
All	881					–0.39	–0.17	0.02	0.19
0–78	100	**.00004**	**2**	**2**	**.001**	—	—	0.02	0.24
78–169	100	**.00288**	1[a]	**2**	**.008**	—	–0.20	0.10	—
169–405	100	**.00515**	1[a]	**2**	**.013**	—	–0.19	0.10	—
405–885	100	**.00042**	**2**	**2**	**.001**	—	–0.25	0.10	—
885–1360	100	**.00029**	**2**	**2**	**.001**	—	–0.25	0.08	—
1360–1785	100	.09739	1	1	.108	—	—	–0.01	—
1785–3142	100	**.00021**	**2**[b]	**4**	**.030**	–0.42	–0.18	–0.01	0.16
3142–4200	100	**.01761**	**2**	**2**	**.006**	–0.30	—	0.00	—
4200–16,712	81	**.04859**	1[a]	**2**	**.030**	–0.30	—	0.00	—

NOTE. Values in boldface indicate nonnormal distributions.
BIC, Bayesian information criterion; LRT, likelihood ratio testing.
[a]Similar BIC values for models with 1 or 2 components.
[b]Similar BIC values for models with 2, 3, or 4 components.

Supplementary Table 2. Host Fecal Calprotectin Distribution in Groups of Specified Microbiota PCoA1 Range

PCoA1 range	Observations, n	Shapiro test for normality, *P*	mclust BIC components, n	mclust LRT components, n	LRT bootstrap, *P*	Mean calprotectin values for components, $\mu g/g$, based on n by LRT				
						1	2	3	4[a]	5[a]
All	881					74	248	1173	3468	6850
0.215 to 0.32	100	**5.7e–12**	**3**	**3**	**.001**	72	308	1536	—	—
0.1552 to 0.215	100	**4.4e–11**	**3**[b]	**5**	**.047**	60	143	923	3023	—
						—	322	—	—	—
0.0999 to 0.1552	100	**2.7e–10**	**3**[c]	**4**	**.025**	90	382	1320	3298	—
0.0413 to 0.0999	100	**3.3e–12**	**3**	**3**	**.001**	123	—	1049	3835	—
–0.006 to 0.0413	100	**1.1e–08**	**4**	**4**	**.001**	84	257	1142	3453	—
–0.0605 to –0.006	100	**8.1e–10**	**6**	**6**	**.008**	63	160	726	3445	8810
						—	—	1598	—	—
–0.156 to –0.0605	100	**5.3e–07**	**3**	**3**	**.001**	—	282	1473	3486	—
–0.288 to –0.156	100	**1.2e–08**	**6**	**6**	**.008**	65	315	1096	3687	7455
						—	—	1893	—	—
–0.53 to –0.288	81	**3.9e–09**	**3**	**3**	**.001**	—	—	911	3546	9144

NOTE. Values in boldface indicate nonnormal distributions.
BIC, Bayesian information criterion; LRT, likelihood ratio testing.
[a]Predicted components 4 and 5 are considered as 1 state (state 4), see Supplementary Figure 2*E* and *F* for explanation.
[b]Similar BIC values for models with 3, 4, or 5 components.
[c]Similar BIC values for models with 3 or 4 components.